Limited Value of Multiparametric MRI with Dynamic Contrast-Enhanced and Diffusion-Weighted Imaging in Non-Mass Enhancing Breast Tumors

Maria Adele Marino[a,b,†], **Daly Avendano**[a,c], **Varadan Sevilmedu**[d], **Sunitha Thakur**[a,e], **Danny Martinez**[a], **Roberto Lo Gullo**[a], **Joao V Horvat**[a], **Thomas H Helbich**[f], **Pascal A T Baltzer**[f], **Katja Pinker**[a,†,*]

[a]Memorial Sloan Kettering Cancer Center, Department of Radiology, Breast Imaging Service, New York, NY, USA

[b]Department of Biomedical Sciences and Morphologic and Functional Imaging, University of Messina, Messina, Italy

[c]Tecnologico de Monterrey, School of Medicine and Health Sciences, Monterrey, Nuevo Leon, Mexico

[d]Memorial Sloan Kettering Cancer Center, Department of Epidemiology and Biostatistics, New York, NY, USA

[e]Department of Medical Physics, Memorial Sloan Kettering Cancer Center, 1275 York Ave, New York, NY 10065, USA

[f]Department of Biomedical Imaging and Image-guided Therapy, Division of Molecular and Structural Preclinical Imaging, Medical University of Vienna, Vienna, Austria

Abstract

Purpose: To investigate the diagnostic value of multiparametric MRI (mpMRI) including dynamic contrast-enhanced magnetic resonance imaging (DCE-MRI) and diffusion-weighted imaging (DWI) in non-mass enhancing breast tumors.

*Correspondence: pinkerdk@mskcc.org; Tel.: +1 646 888 5470.
†Both authors contributed equally

Method: Patients who underwent mpMRI, who were diagnosed with a suspicious non-mass enhancement (NME) on DCE-MRI (BI-RADS 4/5), and who subsequently underwent image-guided biopsy were retrospectively included. Two radiologists independently evaluated all NMEs, on both DCE-MR images and high-b-value DW images. Different mpMRI reading approaches were evaluated: 1) with a fixed apparent diffusion coefficient (ADC) threshold (< 1.3 malignant, 1.3 benign) based on the recommendation by the European Society of Breast Imaging (EUSOBI); 2) with a fixed ADC threshold (< 1.5 malignant,   1.5 benign) based on recently published trial data; 3) with an ADC threshold adapted to the assigned BI-RADS classification using a previously published reading method; and 4) with individually determined best thresholds for each reader.

Results: The final study sample consisted of 66 lesions in 66 patients. DCE-MRI alone had the highest sensitivity for breast cancer detection (94.8–100%), outperforming all mpMRI reading approaches (R1 74.4–87.1%, R2 71.7–94.8%) and DWI alone (R1 74.4%, R2 79.4%). The adapted approach achieved the best specificity for both readers (85.1%), resulting in the best diagnostic accuracy for R1 (86.5%) but a moderate diagnostic accuracy for R2 (77.2%).

Conclusion: mpMRI has limited added diagnostic value to DCE-MRI in the assessment of NME.

Keywords

Introduction

Among current imaging techniques, dynamic contrast-enhanced magnetic resonance imaging (DCE-MRI) of the breast has the highest sensitivity to detect breast cancer [1–5]. However, the high sensitivity of DCE-MRI leads also to the detection of enhancing lesions that are benign rather than malignant, resulting in unnecessary biopsies and follow-up examinations [6,7]. This is especially true for non-mass enhancement (NME) lesions compared with masses, wherein up to 63% of NME lesions are classified as suspicious or highly suspicious for malignancy [8,9].

According to the Breast Imaging Report and Data System (BI-RADS), an NME is defined as an area of enhancement on DCE-MRI that is neither a mass nor a focus and may have areas or spots of normal fibroglandular tissue (FGT) or fat interspersed in the enhancing abnormality [10]. NME may be limited to a small area within one quadrant or extend over small or large regions. Compared to masses, the internal enhancement characteristics of an NME is less informative for malignancy. While the frequency of NME lesions is much lower than that of masses on DCE-MRI (13% versus 76%), it is important to note that NME is the most common presentation for ductal carcinoma in situ (DCIS) and non-palpable invasive cancers [11,12]. NME may also be associated with high-risk lesions and benign conditions such as fibrocystic disease and hormonal changes [13,14]. Therefore, NME poses a challenge to breast DCE-MRI [15–17].

To improve specificity, several functional techniques have been explored, from which diffusion-weighted imaging (DWI) has emerged as being the most clinically useful [18–21].

DWI with apparent diffusion coefficient (ADC) mapping consistently improves specificity for the differentiation of benign and malignant breast tumors [22,23], thus obviating unnecessary breast biopsies [24–26], and is now a recommended technique along with DCE-MRI within a clinical multiparametric MRI (mpMRI) approach [18,27]. However, the literature is scarce on the diagnostic value of mpMRI incorporating DWI in the clinical setting for NME. Findings from a recent study suggested that DWI has limited diagnostic accuracy for lesions presenting as NME on DCE-MRI [28]. In addition, it remains unclear whether recommended ADC thresholds for masses can be translated to NME lesions and used within a multiparametric framework. Therefore, more data about the use of mpMRI to differentiate benign from malignant NME lesions is warranted [8].

The aim of this study was to investigate the diagnostic value of mpMRI including DCE-MRI and DWI in NME lesions.

Material and Methods

Study Sample

This retrospective single-center study was approved by the institutional review board. Some patients were previously analyzed and reported in a different context [28].

We included consecutive patients who met the following inclusion criteria: 1) underwent mpMRI including DCE and DWI as a result of a suspicious abnormality on conventional imaging, 2) were diagnosed with suspicious NME on DCE-MRI (BI-RADS 4/5), and 3) subsequently underwent image-guided breast biopsy between September 2007 and July 2013. Of 95 patients who met the inclusion criteria, 29 patients were excluded due to non-visibility of their NME lesions on DWI and ADC maps (n = 24; 12 benign and 12 malignant) or non-diagnostic quality of DWI (n = 5; 1 benign and 4 malignant) as determined by the study supervisor (**). Among the non-visible NME lesions on DWI, there were 8 DCIS lesions, 3 invasive lobular carcinomas, and 1 invasive ductal carcinoma.

Patient electronic medical records were reviewed for histopathology results; for malignant lesions, these included tumor grade, subtype, and receptor status.

Multiparametric MRI Technique

All patients underwent 3T MRI (Tim Trio, Siemens Erlangen, Germany) using a 4-channel breast coil (in Vivo, Orlando, FL, USA) while lying in the prone position. The mpMRI protocol is summarized in Table 1. [26,29–31]. According to literature [31] , the DCE-MRI sequences were isotropic and subsequently reformatted in axial and sagittal plane. Gadoteratemeglumine (Gd-DOTA;Dotarem®, Guerbet, France) was injected intravenously as a bolus (0.1 mmol/kg body weight) using a power injector (Spectris Solaris EP, Medrad, Pittsburgh, PA, USA) at a rate of 4 ml/s, followed by a 20-ml saline flush. The contrast agent was injected 75 s after starting the first coronal T1-weighted VIBE. The total examination time of the mpMRI imaging protocol was 18:40 min.

Imaging Assessment

All NME lesions were independently assessed by two breast imaging radiologists (**, **), with 6 and 4 years of experience on Breast MRI, respectively, who were blinded to BI-RADS assignment on conventional imaging, BI-RADS assignment on DCE-MRI, as well as the final histopathological diagnosis but were aware that each patient had an NME that was classified as suspicious (BI-RADS 4/5) on clinical interpretation. There was a wash-out period between readings for each reader of at least three weeks. Each reader independently assessed the following lesion characteristics on DCE-MRI according to BI-RADS: a) distribution, b) internal enhancement patterns, and c) symmetry. Each reader also assigned a BI-RADS category to each NME lesion on DCE-MRI after evaluating the semi-quantitative kinetics of NME in the initial and delayed phase according to BI-RADS, by region of interest (ROI) placement.

Subsequently, each reader assessed high-b-value (i.e., 850 s/mm^2) DW axial images for hyperintense regions corresponding to enhancing lesions on DCE-MRI. The mean ADC of each lesion was determined by manually placing a circular 10 mm focused 2D ROI selecting the lowest ADC value within the enhancing lesion, i.e., the most suspicious area, avoiding vessels and necrosis areas. To account for possible inter-reader variability, the readers were instructed to repeat all measurements twice and the lowest ADC value was recorded.

Four different mpMRI reading approaches were evaluated:

1. The European Society of Breast Imaging (EUSOBI) mpMRI: using a fixed ADC mean threshold (< 1.3 malignant,   1.3 benign) as proposed by the European Society of Breast Imaging International Breast Diffusion-Weighted Imaging working group [18]

2. 1.5 mpMRI: using a fixed ADC mean threshold (< 1.5 malignant,   1.5 benign) as proposed and validated recently [19,32]

3. Adapted mpMRI: using an ADC mean threshold adapted to the assigned BI-RADS classification based on a previously developed method to efficiently combine the parameters gathered from both DCE-MRI and DWI [29]

4. mpMRI individual threshold: using the best threshold of ADC mean for each reader in differentiating between benign and malignant NME was determined

Histopathology

Histopathological diagnosis served as the reference standard. In the case of a benign diagnosis at image-guided needle biopsy, the final diagnosis was benign. In the case of a high-risk lesion with uncertain potential for malignancy, the final diagnosis was established by surgery. All malignant lesions underwent surgical excision before or after neoadjuvant treatment per the treating physician's preference. In the case of upfront surgical excision, the final histopathological diagnosis was obtained from the surgical specimen, whereas in the case of surgical excision after neoadjuvant treatment, the final histopathological diagnosis was obtained from the biopsy specimen.

Statistical Analysis

All statistical analyses were performed using R 3.6.3. The best individual ADC mean threshold for each reader in differentiating between benign and malignant NME lesions was calculated using Youden's index. Sensitivity, specificity, positive predictive value (PPV), negative predictive value (NPV), and accuracy were determined for DCE-MRI alone, DWI using the best individual ADC mean thresholds, and all different mpMRI reading approaches, with corresponding 95% exact confidence intervals (CIs). Comparisons of sensitivity, specificity, and accuracy between DCE-MRI, EUSOBI mpMRI, 1.5 mpMRI, adapted mpMRI, and mpMRI individual threshold approaches were performed using the McNemar's test. Multiple comparison correction was performed using Bonferroni procedure. Inter-rater agreement was estimated using the κ statistic. Type I error for all statistical tests was set to 0.05 (α).

Results

Patient and Lesion Characteristics

The final study sample consisted of 66 patients (65 women, 1 man; mean age = 51.8 ± 10.8 years, range 26–76 years).

Histopathological characteristics of the study sample are summarized in Table 2. Of the 66 NME lesions (mean size 40 ± 25 mm, range 5–98 mm) detected on DCE-MRI, 39/66 (59%) were malignant (mean size 48.4 ± 26 mm, range, 5–98 mm) and 27/66 (41%) were benign (mean size 27.8 ± 18.3, range 5–80 mm). The lesions were measured considering the largest diameter in axial plane on DCE-MRI sequences.

On DCE-MRI, among benign lesions, the most frequent enhancement distribution was focal (13/27, 48%) and the majority had a homogenous pattern of internal enhancement (15/27, 56%).

The majority of benign NME lesions demonstrated slow or medium enhancement in the early phase (20/27, 74%) and persistent or plateau enhancement in the delayed phase (26/27, 97%) , while only 7/27 (26%) showed a fast-early enhancement with only sclerosing adenosis 1/27 (3%) demonstrating wash-out in the delayed phase. Among malignant lesions, most NME lesions had homogenous internal enhancement (17/39, 44%) with even distribution between regional and focal enhancement (both 9/39, 23%). Most of the malignant lesions presented with a fast-early enhancement (26/39,67%) and plateau (18/39,46%) in the delayed enhancing phase. In Table 3, frequencies of NME features on DCE-MRI according to the BI-RADS lexicon are presented.

On DWI, benign lesions presented with a mean ADC value > 1.4 mm^2/s for both readers while malignant lesions with a mean ADC value < 1.2×10^{-3} mm^2/s. The lowest value for a benign lesion was 0.71 (R1) corresponding to adenosis and 1.13 (R2) corresponding to fat necrosis. For malignant lesions, the highest value acquired was 1.71 (R1) corresponding to invasive ductal carcinoma (IDC) and 1.65 (R2) corresponding to invasive lobular carcinoma. Means and ranges of ADC for benign and malignant lesions are listed in Table 4.

Diagnostic Metrics

Sensitivity, specificity, PPV, NPV, diagnostic accuracy, and area under the curve (AUC) for DCE, DWI using the determined best cut-off for each reader, and each mpMRI reading approach (EUSOBI mpMRI, 1.5 mpMRI, adapted mpMRI, and mpMRI individual threshold) for both readers are summarized in Table 5. All significant findings are before multiple comparison adjustments.

For DWI using the determined best cut-off for each reader, the best ADC mean threshold for R1 was 1.215, at which sensitivity was 74.36%, specificity 66.66%, PPV 76.34%, NPV 64.24%, diagnostic accuracy 71.28%, and AUC 0.753 (Figure 1). The best ADC mean threshold for R2 was 1.305, at which sensitivity was 79.42%, specificity 81.40%, PPV 86.02%, NPV 73.26%, diagnostic accuracy 80.3%, and AUC 0.873.

DCE-MRI was the most sensitive technique for breast cancer detection, with sensitivities of 94.82% (R1) and 100% (R2), outperforming all mpMRI approaches with sensitivities ranging from 74.36–87.12% (R1) and 71.72–94.82% (R2) as well as DWI with sensitivities of 74.36% (R1) and 79.42% (R2). The sensitivities of mpMRI using the individual readers' thresholds were significantly different from that of DCE-MRI. DCE-MRI had limited specificities of 66.66% (R1) and 77.88% (R2), albeit resulting in good diagnostic accuracies of 83.38 (R1) and 90.86 (R2) and the lowest number of false negatives (2 for R1; 0 for R2), compared with all mpMRI approaches and DWI. The adapted mpMRI reading approach achieved the best specificity for both readers (85.14% for both R1 and R2) resulting in the best diagnostic accuracy of 86.46% for R1 but a moderate diagnostic accuracy of 77.22% for R2 (Figure 2). While there was an increase in specificity with all mpMRI reading approaches for R2 except 1.5 mpMRI, compared with DCE-MRI, the specificity only increased with adapted mpMRI for R1. For both readers, the least valuable mpMRI reading approach was that of 1.5 mpMRI, with specificities ranging from 29.7–40.7%, which were significantly different from the specificities of DCE-MRI as well as that of all other mpMRI approaches. Except for the adapted mpMRI approach for R1, diagnostic accuracies for all mpMRI approaches and DWI were inferior to diagnostic accuracies of DCE-MRI, with significant differences for (R1) EUSOBI and 1.5 mpMRI and for (R2) EUSOBI, 1.5 mpMRI, and adapted mpMRI.

False positive and false negative results for DCE-MRI, DWI using the determined best cut-off of each reader, EUSOBI mpMRI, 1.5 mpMRI, adapted mpMRI, and mpMRI individual threshold for each reader are listed in Table 6.

There was almost perfect inter-reader agreement for DCE-MRI readings with $\kappa = 1$, and there was moderate inter-rater agreement for the adapted mpMRI assessment, with $\kappa = 0.51$. The agreement was poor ($\kappa < 0.4$) for EUSOBI mpMRI, 1.5 mpMRI, and mpMRI individual threshold approaches.

The readers achieved almost perfect agreement when classifying the NME lesions using the BI-RADS descriptors with k ranging between 0.91 and 1.

Discussion

In this study, we investigated the diagnostic value of mpMRI including DCE-MRI and DWI in NME breast lesions, comparing different mpMRI reading approaches as well as between different mpMRI approaches, DCE-MRI alone, and DWI alone. We demonstrated that while mpMRI may improve the specificity of breast cancer detection in NME lesions, with the adapted mpMRI reading approach being the most valuable approach, this comes at the expense of sensitivity and overall diagnostic accuracy. DCE-MRI remains the most sensitive and accurate modality for NME breast cancer detection.

Breast lesions presenting as NME on DCE-MRI are a diagnostic dilemma for breast radiologists, especially in terms of the sensitivity and specificity of DCE-MRI for these lesions. Previous studies investigating DWI with ADC mapping for the assessment of breast lesions, which included mainly masses and fewer NME lesions, reported sensitivities of up to 96% and specificities of up to 100% [25,29,33]. While it is clear in enhancing masses that mpMRI improves specificity and diagnostic accuracy for breast cancer detection and can reduce the number of unnecessary biopsy recommendations [19,22,25,29,34–44], there is suspicion that mpMRI is not as useful for the differentiation of benign and malignant NME lesions. The results of our study confirm that the diagnostic value of mpMRI in NME lesions is limited, which is conclusive since prior data that have investigated the value of DWI alone in NME lesions yielded similar results. It must also be noted that in a significant number of both benign and malignant lesions, the NME lesions visible on DCE-MRI cannot be distinguished on DWI and are thus not amendable to any diagnostic mpMRI approach.

The accuracy of DWI with ADC mapping is limited in breast tumors presenting as NME lesions with best results being achieved on invasive cancers. Up to a third of NMEs cannot be evaluated with DWI, and therefore DWI with ADM mapping seems at present not sufficient for early detection of DCIS.

We aimed to fully elucidate the potential of mpMRI for the assessment of NME lesions. For DWI, we employed the previously recommended ROI measurement approach, using a 10-mm focused 2D ROI selecting the lowest ADC value within the enhancing lesion, i.e., the most suspicious area, and ADC mean for lesion assessment; subsequently, we investigated different proposed mpMRI approaches [28]. An ADC mean threshold < 1.3, which is considered a suspicious diffusion hindrance level according to the EUSOBI DWI working group consensus paper [18]; an ADC threshold of 1.5 based on multicenter studies [19,32]; a threshold specifically for NME lesions adapted to the assigned BI-RADS classification [29]; and the best individual threshold of ADC mean for the differentiation of benign and malignant NME lesions determined for each reader were evaluated.

Our results indicate that for the assessment of NME, DCE is superior and the diagnostic value of mpMRI across reading approaches is limited; moreover, previously recommended ADC thresholds for masses cannot seamlessly be extrapolated to NME lesions. In particular, in agreement with Clauser et al. [19,32], the recent conservative ADC threshold of 1.5, which aimed at maximizing sensitivity while maintaining good specificity to obviate unnecessary breast biopsies in benign breast lesions, did not deliver in NME lesions. While

the 1.5 mpMRI approach achieved a sensitivity that was lower but that was not significantly different from that of DCE-MRI, results for specificity were insufficient, ranging as low as 29.7–40.7%. When the 1.5 mpMRI approach was compared with DCE-MRI, false-positive findings increased from 9 to 19 for R1 and from 6 to 16 for R2, corresponding to a rate of unnecessary breast biopsies that is not appropriate in clinical practice. While this increase was less pronounced for the other mpMRI approaches for R1, and a reduction of false-positive results was even shown for R2, the added specificity came at the expense of sensitivity, resulting in overall lower diagnostic accuracy.

The adapted mpMRI reading approach, where the threshold is adapted to the assigned BI-RADS classification, was the most useful mpMRI reading approach to improve specificity to obviate unnecessary biopsies. The application of a flexible "traffic light" threshold was first proposed by Baltzer et al., showing that the integration of quantitative ADC values by the means of a simple sum score into the clinical reading of DCE-MRI of the breast improves specificity in depicting malignancies, achieving a sensitivity of 100% and a specificity up to 92.4% [30]. Pinker et al. then developed a BI-RADS-adapted reading approach for mpMRI of the breast using DCE-MRI and DWI that adapted ADC thresholds to the assigned BI-RADS classification. The developed BI-RADS-adapted reading approach maintained excellent sensitivity (96.2%) while significantly increasing the specificity from 70.6% to 89.4%, equaling that of DWI [29]. It has to be noted that in both these studies, which achieved better results than our study, the majority of breast tumors were masses and no subgroup analysis for NME lesions was performed. While there is clear evidence that mpMRI improves diagnostic accuracy, for NME lesions, the afforded benefit in the increase in specificity is not as high and may even negatively impact sensitivity. This finding highlights the importance of the necessity to consciously combine the morphologic and functional information afforded by DCE-MRI with DWI. Moreover, our results indicate that when DCE-MRI is suggestive of breast cancer, this should take precedence over DWI and biopsy should be recommended.

Since the role of MRI for the detection and management of breast cancer continues to evolve, with a growing number of studies indicating that it could be an important method for screening in an expanded population of women [45–49], along with the fact that DWI is nowadays an essential part of the multiparametric breast MRI protocol [18], it is important to be aware of its current limitations. The sensitivity of DWI and subsequently of mpMRI including DCE and DWI is limited in lesions 12 mm or lesions presenting as diffuse NME [33]. However, research to improve the spatial resolution of DWI is ongoing. Hence, it can be expected that further advances are possible to overcome its current limitations.

In our study, we found almost perfect inter-reader agreement for DCE-MRI ($\kappa = 1$) while it was only moderate for the adapted mpMRI reading approach ($\kappa = 0.5$) and poorer for all other mpMRI approaches. The results of the study are in good agreement with prior work [28] and shows that differences between readers exist and that readers benefit differently from mpMRI, which is most likely due to different ROI selections for the measurement of ADC values.

Some potential limitations of our study merit consideration. First, we included patients who underwent MRI examination of the breast and subsequently biopsy as part of their clinical care (BI-RADS 4/5). In doing so, we might have encountered a pre-selection criteria bias. Other limitations of our study are the single-institution and retrospective study design as well as the small number of cases; thus, our findings need to be verified in larger-scale studies. However, this is one of the largest cohorts of NME breast lesions so far presented in the literature.

Novel methods such as radiomics and neural networks have been used recently in different breast diagnostic scenarios, with interesting results. Li et al. assessed the additional value of a radiomics-based signature to distinguish between benign and malignant NME lesions on breast DCE-MRI. Their radiomic model with six features was significantly correlated with malignancy (p < 0.001). The model combining radiomic signatures and time-intensity curve type achieved a sensitivity of 82% and a specificity of 86.4% in the validation cohort [50]. Wang et al. developed an artificial intelligence (AI) system to classify benign and malignant NME lesions using maximum intensity projection (MIP) images of early post-contrast subtracted breast MRI. The AI system yielded an AUC of 0.859 and 0.816 in test sets A and B, respectively, showing comparable performance to the senior radiologist (p = 0.558 and 0.041) and outperforming the junior radiologist (p < 0.001 and 0.009) in both test sets. With the aid of the AI system, the AUC of the junior radiologist increased in both test sets A and B, from 0.740 to 0.862 (p < 0.001) and from 0.732 to 0.843 (p < 0.001), respectively [51].

Conclusions

In conclusion, the diagnostic value of mpMRI in the assessment of NME lesions is limited. While mpMRI may improve the specificity of breast cancer detection in NME lesions, with an mpMRI BI-RADS adapted reading approach as the most valuable reading approach, this comes at the expense of sensitivity and overall diagnostic accuracy. In NME lesions, DCE remains the most sensitive and most accurate modality for breast cancer detection.

Acknowledgments

Abbreviations:

ADC	apparent diffusion coefficient
AUC	area under the curve
BI-RADS	Breast Imaging Report and Data System

CI	confidence interval
DCE-MRI	dynamic contrast-enhanced magnetic resonance imaging
DCIS	ductal carcinoma in situ
DWI	diffusion-weighted imaging
EUSOBI	European Society of Breast Imaging
FGT	fibroglandular tissue
FOV	field of view
MIP	maximum intensity projection
mpMRI	multiparametric magnetic resonance imaging
NME	non-mass enhancement
NPV	negative predictive value
PPV	positive predictive value
ROI	region of interest

References

[1]. Pinker K, Helbich TH, Morris EA, The potential of multiparametric MRI of the breast, Br. J. Radiol 90 (2017) 20160715. 10.1259/bjr.20160715. [PubMed: 27805423]

[2]. Marino MA, Helbich T, Baltzer P, Pinker-Domenig K, Multiparametric MRI of the breast: A review, J. Magn. Reson. Imaging JMRI 47 (2018) 301–315. 10.1002/jmri.25790. [PubMed: 28639300]

[3]. Mann RM, Cho N, Moy L, Breast MRI: State of the Art, Radiology 292 (2019) 520–536. 10.1148/radiol.2019182947. [PubMed: 31361209]

[4]. Mann RM, Balleyguier C, Baltzer PA, Bick U, Colin C, Cornford E, Evans A, Fallenberg E, Forrai G, Fuchsjäger MH, Gilbert FJ, Helbich TH, Heywang-Köbrunner SH, Camps-Herrero J, Kuhl CK, Martincich L, Pediconi F, Panizza P, Pina LJ, Pijnappel RM, Pinker-Domenig K, Skaane P, Sardanelli F, European Society of Breast Imaging (EUSOBI), with language review by Europa Donna–The European Breast Cancer Coalition, Breast MRI: EUSOBI recommendations for women's information, Eur. Radiol 25 (2015) 3669–3678. 10.1007/s00330-015-3807-z. [PubMed: 26002130]

[5]. Leithner D, Wengert GJ, Helbich TH, Thakur S, Ochoa-Albiztegui RE, Morris EA, Pinker K, Clinical role of breast MRI now and going forward, Clin. Radiol 73 (2018) 700–714. 10.1016/j.crad.2017.10.021. [PubMed: 29229179]

[6]. Baltzer PAT, Kaiser WA, Dietzel M, Lesion type and reader experience affect the diagnostic accuracy of breast MRI: a multiple reader ROC study, Eur. J. Radiol 84 (2015) 86–91. 10.1016/j.ejrad.2014.10.023. [PubMed: 25466772]

[7]. Spick C, Szolar DHM, Preidler KW, Tillich M, Reittner P, Baltzer PA, Breast MRI used as a problem-solving tool reliably excludes malignancy, Eur. J. Radiol 84 (2015) 61–64. 10.1016/j.ejrad.2014.10.005. [PubMed: 25454098]

[8]. Gity M, Ghazi Moghadam K, Jalali AH, Shakiba M, Association of Different MRI BIRADS Descriptors With Malignancy in Non Mass-Like Breast Lesions, Iran. Red Crescent Med. J 16 (2014). 10.5812/ircmj.26040.

[9]. Tozaki M, Fukuda K, High-spatial-resolution MRI of non-masslike breast lesions: interpretation model based on BI-RADS MRI descriptors, AJR Am. J. Roentgenol 187 (2006) 330–337. 10.2214/ajr.187.3.w330. [PubMed: 16861534]

[10]. American College of Radiology BI-RADS Atlas (2013), 5th Edition., (n.d.). https://www.acr.org/Clinical-Resources/Reporting-and-Data-Systems/Bi-Rads (accessed May 15, 2018).

[11]. Yang Q-X, Ji X, Feng L-L, Zheng L, Zhou X-Q, Wu Q, Chen X, Significant MRI indicators of malignancy for breast non-mass enhancement, J. X-Ray Sci. Technol 25 (2017) 1033–1044. 10.3233/XST-17311.

[12]. Gutierrez RL, DeMartini WB, Eby PR, Kurland BF, Peacock S, Lehman CD, BI-RADS lesion characteristics predict likelihood of malignancy in breast MRI for masses but not for nonmasslike enhancement, AJR Am. J. Roentgenol 193 (2009) 994–1000. 10.2214/AJR.08.1983. [PubMed: 19770321]

[13]. Newstead GM, MR imaging of ductal carcinoma in situ, Magn. Reson. Imaging Clin. N. Am 18 (2010) 225–240, viii. 10.1016/j.mric.2010.02.004. [PubMed: 20494308]

[14]. Greenwood HI, Heller SL, Kim S, Sigmund EE, Shaylor SD, Moy L, Ductal carcinoma in situ of the breasts: review of MR imaging features, Radiogr. Rev. Publ. Radiol. Soc. N. Am. Inc 33 (2013) 1569–1588. 10.1148/rg.336125055.

[15]. Baltzer PAT, Benndorf M, Dietzel M, Gajda M, Runnebaum IB, Kaiser WA, False-positive findings at contrast-enhanced breast MRI: a BI-RADS descriptor study, AJR Am. J. Roentgenol 194 (2010) 1658–1663. 10.2214/AJR.09.3486. [PubMed: 20489110]

[16]. Benndorf M, Baltzer PAT, Kaiser WA, Assessing the degree of collinearity among the lesion features of the MRI BI-RADS lexicon, Eur. J. Radiol 80 (2011) e322–324. 10.1016/j.ejrad.2010.11.030. [PubMed: 21193277]

[17]. Jansen SA, Shimauchi A, Zak L, Fan X, Karczmar GS, Newstead GM, The diverse pathology and kinetics of mass, nonmass, and focus enhancement on MR imaging of the breast, J. Magn. Reson. Imaging JMRI 33 (2011) 1382–1389. 10.1002/jmri.22567. [PubMed: 21591007]

[18]. Baltzer P, Mann RM, Iima M, Sigmund EE, Clauser P, Gilbert FJ, Martincich L, Partridge SC, Patterson A, Pinker K, Thibault F, Camps-Herrero J, Le Bihan D, EUSOBI international Breast Diffusion-Weighted Imaging working group, Diffusion-weighted imaging of the breast-a consensus and mission statement from the EUSOBI International Breast Diffusion-Weighted Imaging working group, Eur. Radiol 30 (2020) 1436–1450. 10.1007/s00330-019-06510-3. [PubMed: 31786616]

[19]. Rahbar H, Zhang Z, Chenevert TL, Romanoff J, Kitsch AE, Hanna LG, Harvey SM, Moy L, DeMartini WB, Dogan B, Yang WT, Wang LC, Joe BN, Oh KY, Neal CH, McDonald ES, Schnall MD, Lehman CD, Comstock CE, Partridge SC, Utility of Diffusion-weighted Imaging to Decrease Unnecessary Biopsies Prompted by Breast MRI: A Trial of the ECOG-ACRIN Cancer Research Group (A6702), Clin. Cancer Res. Off. J. Am. Assoc. Cancer Res 25 (2019) 1756–1765. 10.1158/1078-0432.CCR-18-2967.

[20]. Partridge SC, Amornsiripanitch N, DWI in the Assessment of Breast Lesions, Top. Magn. Reson. Imaging TMRI 26 (2017) 201–209. 10.1097/RMR.0000000000000137. [PubMed: 28961569]

[21]. Partridge SC, Nissan N, Rahbar H, Kitsch AE, Sigmund EE, Diffusion-weighted breast MRI: Clinical applications and emerging techniques, J. Magn. Reson. Imaging JMRI 45 (2017) 337–355. 10.1002/jmri.25479. [PubMed: 27690173]

[22]. Partridge SC, DeMartini WB, Kurland BF, Eby PR, White SW, Lehman CD, Quantitative diffusion-weighted imaging as an adjunct to conventional breast MRI for improved positive predictive value, AJR Am. J. Roentgenol 193 (2009) 1716–1722. 10.2214/AJR.08.2139. [PubMed: 19933670]

[23]. Kul S, Cansu A, Alhan E, Dinc H, Gunes G, Reis A, Contribution of diffusion-weighted imaging to dynamic contrast-enhanced MRI in the characterization of breast tumors, AJR Am. J. Roentgenol 196 (2011) 210–217. 10.2214/AJR.10.4258. [PubMed: 21178069]

[24]. Baltzer PAT, Benndorf M, Dietzel M, Gajda M, Camara O, Kaiser WA, Sensitivity and specificity of unenhanced MR mammography (DWI combined with T2-weighted TSE imaging, ueMRM) for the differentiation of mass lesions, Eur. Radiol 20 (2010) 1101–1110. 10.1007/s00330-009-1654-5. [PubMed: 19936758]

[25]. Spick C, Pinker-Domenig K, Rudas M, Helbich TH, Baltzer PA, MRI-only lesions: application of diffusion-weighted imaging obviates unnecessary MR-guided breast biopsies, Eur. Radiol 24 (2014) 1204–1210. 10.1007/s00330-014-3153-6. [PubMed: 24706105]

[26]. Pinker K, Bogner W, Baltzer P, Gruber S, Bickel H, Brueck B, Trattnig S, Weber M, Dubsky P, Bago-Horvath Z, Bartsch R, Helbich TH, Improved diagnostic accuracy with multiparametric magnetic resonance imaging of the breast using dynamic contrast-enhanced magnetic resonance imaging, diffusion-weighted imaging, and 3-dimensional proton magnetic resonance spectroscopic imaging, Invest. Radiol 49 (2014) 421–430. 10.1097/RLI.0000000000000029. [PubMed: 24566292]

[27]. Daimiel Naranjo I, Lo Gullo R, Saccarelli C, Thakur SB, Bitencourt A, Morris EA, Jochelson MS, Sevilimedu V, Martinez DF, Pinker-Domenig K, Diagnostic value of diffusion-weighted imaging with synthetic b-values in breast tumors: comparison with dynamic contrast-enhanced and multiparametric MRI, Eur. Radiol 31 (2021) 356–367. 10.1007/s00330-020-07094-z. [PubMed: 32780207]

[28]. Avendano D, Marino MA, Leithner D, Thakur S, Bernard-Davila B, Martinez DF, Helbich TH, Morris EA, Jochelson MS, Baltzer PAT, Clauser P, Kapetas P, Pinker K, Limited role of DWI with apparent diffusion coefficient mapping in breast lesions presenting as non-mass enhancement on dynamic contrast-enhanced MRI, Breast Cancer Res. BCR 21 (2019) 136. 10.1186/s13058-019-1208-y. [PubMed: 31801635]

[29]. Pinker K, Bickel H, Helbich TH, Gruber S, Dubsky P, Pluschnig U, Rudas M, Bago-Horvath Z, Weber M, Trattnig S, Bogner W, Combined contrast-enhanced magnetic resonance and diffusion-weighted imaging reading adapted to the "Breast Imaging Reporting and Data System" for multiparametric 3-T imaging of breast lesions, Eur. Radiol 23 (2013) 1791–1802. 10.1007/s00330-013-2771-8. [PubMed: 23504036]

[30]. Bogner W, Gruber S, Pinker K, Grabner G, Stadlbauer A, Weber M, Moser E, Helbich TH, Trattnig S, Diffusion-weighted MR for differentiation of breast lesions at 3.0 T: how does selection of diffusion protocols affect diagnosis?, Radiology 253 (2009) 341–351. 10.1148/radiol.2532081718. [PubMed: 19703869]

[31]. Pinker K, Grabner G, Bogner W, Gruber S, Szomolanyi P, Trattnig S, Heinz-Peer G, Weber M, Fitzal F, Pluschnig U, Rudas M, Helbich T, A combined high temporal and high spatial resolution 3 Tesla MR imaging protocol for the assessment of breast lesions: initial results, Invest. Radiol 44 (2009) 553–558. 10.1097/RLI.0b013e3181b4c127. [PubMed: 19652611]

[32]. Clauser P, Krug B, Bickel H, Dietzel M, Pinker K, Neuhaus V-F, Marino MA, Moschetta M, Troiano N, Helbich TH, Baltzer PAT, Diffusion-weighted Imaging Allows for Downgrading MR BI-RADS 4 Lesions in Contrast-enhanced MRI of the Breast to Avoid Unnecessary Biopsy, Clin. Cancer Res. Off. J. Am. Assoc. Cancer Res 27 (2021) 1941–1948. 10.1158/1078-0432.CCR-20-3037.

[33]. Pinker K, Moy L, Sutton EJ, Mann RM, Weber M, Thakur SB, Jochelson MS, Bago-Horvath Z, Morris EA, Baltzer PA, Helbich TH, Diffusion-Weighted Imaging With Apparent Diffusion Coefficient Mapping for Breast Cancer Detection as a Stand-Alone Parameter: Comparison With Dynamic Contrast-Enhanced and Multiparametric Magnetic Resonance Imaging, Invest. Radiol 53 (2018) 587–595. 10.1097/RLI.0000000000000465. [PubMed: 29620604]

[34]. Baltzer A, Dietzel M, Kaiser CG, Baltzer PA, Combined reading of Contrast Enhanced and Diffusion Weighted Magnetic Resonance Imaging by using a simple sum score, Eur. Radiol 26 (2016) 884–891. 10.1007/s00330-015-3886-x. [PubMed: 26115653]

[35]. Woodhams R, Matsunaga K, Iwabuchi K, Kan S, Hata H, Kuranami M, Watanabe M, Hayakawa K, Diffusion-weighted imaging of malignant breast tumors: the usefulness of apparent diffusion coefficient (ADC) value and ADC map for the detection of malignant breast tumors and evaluation of cancer extension, J. Comput. Assist. Tomogr 29 (2005) 644–649. 10.1097/01.rct.0000171913.74086.1b. [PubMed: 16163035]

[36]. Woodhams R, Matsunaga K, Kan S, Hata H, Ozaki M, Iwabuchi K, Kuranami M, Watanabe M, Hayakawa K, ADC mapping of benign and malignant breast tumors, Magn. Reson. Med. Sci. MRMS Off. J. Jpn. Soc. Magn. Reson. Med 4 (2005) 35–42. 10.2463/mrms.4.35.

[37]. Rubesova E, Grell A-S, De Maertelaer V, Metens T, Chao S-L, Lemort M, Quantitative diffusion imaging in breast cancer: a clinical prospective study, J. Magn. Reson. Imaging JMRI 24 (2006) 319–324. 10.1002/jmri.20643. [PubMed: 16786565]

[38]. Wenkel E, Geppert C, Schulz-Wendtland R, Uder M, Kiefer B, Bautz W, Janka R, Diffusion weighted imaging in breast MRI: comparison of two different pulse sequences, Acad. Radiol. 14 (2007) 1077–1083. 10.1016/j.acra.2007.06.006. [PubMed: 17707315]

[39]. Baltzer P. a. T., Renz DM, Herrmann K-H, Dietzel M, Krumbein I, Gajda M, Camara O, Reichenbach JR, Kaiser WA, Diffusion-weighted imaging (DWI) in MR mammography (MRM): clinical comparison of echo planar imaging (EPI) and half-Fourier single-shot turbo spin echo (HASTE) diffusion techniques, Eur. Radiol 19 (2009) 1612–1620. 10.1007/s00330-009-1326-5. [PubMed: 19288109]

[40]. Chen X, Li W, Zhang Y, Wu Q, Guo Y, Bai Z, Meta-analysis of quantitative diffusion-weighted MR imaging in the differential diagnosis of breast lesions, BMC Cancer 10 (2010) 693. 10.1186/1471-2407-10-693. [PubMed: 21189150]

[41]. Dorrius MD, Dijkstra H, Oudkerk M, Sijens PE, Effect of b value and pre-admission of contrast on diagnostic accuracy of 1.5-T breast DWI: a systematic review and meta-analysis, Eur. Radiol 24 (2014) 2835–2847. 10.1007/s00330-014-3338-z. [PubMed: 25103535]

[42]. Shi R-Y, Yao Q-Y, Wu L-M, Xu J-R, Breast Lesions: Diagnosis Using Diffusion Weighted Imaging at 1.5T and 3.0T-Systematic Review and Meta-analysis, Clin. Breast Cancer 18 (2018) e305–e320. 10.1016/j.clbc.2017.06.011. [PubMed: 28802529]

[43]. Iima M, Kataoka M, Kanao S, Onishi N, Kawai M, Ohashi A, Sakaguchi R, Toi M, Togashi K, Intravoxel Incoherent Motion and Quantitative Non-Gaussian Diffusion MR Imaging: Evaluation of the Diagnostic and Prognostic Value of Several Markers of Malignant and Benign Breast Lesions, Radiology 287 (2018) 432–441. 10.1148/radiol.2017162853. [PubMed: 29095673]

[44]. Iima M, Yano K, Kataoka M, Umehana M, Murata K, Kanao S, Togashi K, Le Bihan D, Quantitative non-Gaussian diffusion and intravoxel incoherent motion magnetic resonance imaging: differentiation of malignant and benign breast lesions, Invest. Radiol 50 (2015) 205–211. 10.1097/RLI.0000000000000094. [PubMed: 25260092]

[45]. Monticciolo DL, Newell MS, Moy L, Niell B, Monsees B, Sickles EA, Breast Cancer Screening in Women at Higher-Than-Average Risk: Recommendations From the ACR, J. Am. Coll. Radiol. JACR 15 (2018) 408–414. 10.1016/j.jacr.2017.11.034. [PubMed: 29371086]

[46]. Kuhl CK, Strobel K, Bieling H, Leutner C, Schild HH, Schrading S, Supplemental Breast MR Imaging Screening of Women with Average Risk of Breast Cancer, Radiology 283 (2017) 361–370. 10.1148/radiol.2016161444. [PubMed: 28221097]

[47]. Kuhl CK, Schrading S, Strobel K, Schild HH, Hilgers R-D, Bieling HB, Abbreviated breast magnetic resonance imaging (MRI): first postcontrast subtracted images and maximum-intensity projection-a novel approach to breast cancer screening with MRI, J. Clin. Oncol. Off. J. Am. Soc. Clin. Oncol 32 (2014) 2304–2310. 10.1200/JCO.2013.52.5386.

[48]. Bakker MF, de Lange SV, Pijnappel RM, Mann RM, Peeters PHM, Monninkhof EM, Emaus MJ, Loo CE, Bisschops RHC, Lobbes MBI, de Jong MDF, Duvivier KM, Veltman J, Karssemeijer N, de Koning HJ, van Diest PJ, Mali WPTM, van den Bosch MAAJ, Veldhuis WB, van Gils CH, DENSE Trial Study Group, Supplemental MRI Screening for Women with Extremely Dense Breast Tissue, N. Engl. J. Med 381 (2019) 2091–2102. 10.1056/NEJMoa1903986. [PubMed: 31774954]

[49]. Comstock CE, Gatsonis C, Newstead GM, Snyder BS, Gareen IF, Bergin JT, Rahbar H, Sung JS, Jacobs C, Harvey JA, Nicholson MH, Ward RC, Holt J, Prather A, Miller KD, Schnall MD, Kuhl CK, Comparison of Abbreviated Breast MRI vs Digital Breast Tomosynthesis for Breast Cancer Detection Among Women With Dense Breasts Undergoing Screening, JAMA 323 (2020) 746–756. 10.1001/jama.2020.0572. [PubMed: 32096852]

[50]. Li Y, Yang ZL, Lv WZ, Qin YJ, Tang CL, Yan X, Guo YH, Xia LM, Ai T, Non-Mass Enhancements on DCE-MRI: Development and Validation of a Radiomics-Based Signature for Breast Cancer Diagnoses, Front. Oncol 11 (2021) 738330. 10.3389/fonc.2021.738330. [PubMed: 34631572]

[51]. Wang L, Chang L, Luo R, Cui X, Liu H, Wu H, Chen Y, Zhang Y, Wu C, Li F, Liu H, Guan W, Wang D, An artificial intelligence system using maximum intensity projection MR images

facilitates classification of non-mass enhancement breast lesions, Eur. Radiol (2022). 10.1007/s00330-022-08553-5.

Highlights

- mpMRI shows limited diagnostic value in NME lesions

- Across four mpMRI approaches, adapted mpMRI has the highest specificity

- Increases in specificity are at the expense of sensitivity and overall diagnostic accuracy

- DCE-MRI remains the most sensitive and accurate modality for NME breast cancer detection (94.8–100%)
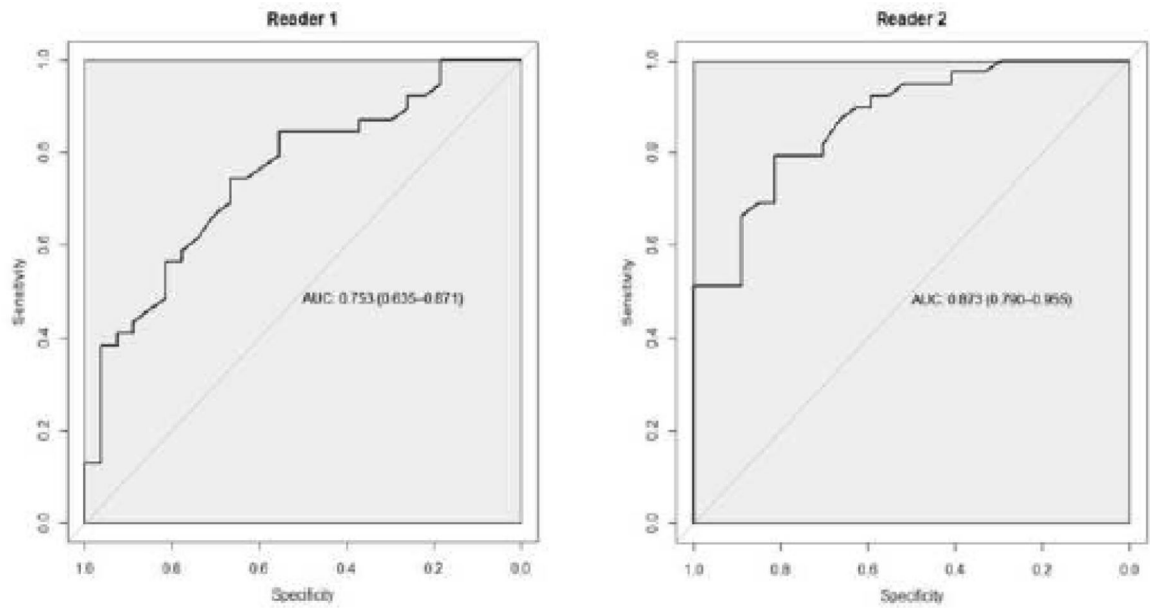
Figure 1.
Receiver operating characteristic curve of ADC for Reader 1 and for Reader 2.

Figure 2.
47-year-old woman who presented on DCE-MRI (A) with a regional heterogenous NME in the right breast that was classified as BI-RADS 3 (R1) and BI-RADS 4 (R2) with high signal intensity on DW images (B) and ADC mean value of $1.241 \times 10^{-3} mm^2/s$ (C). Histopathology from image-guide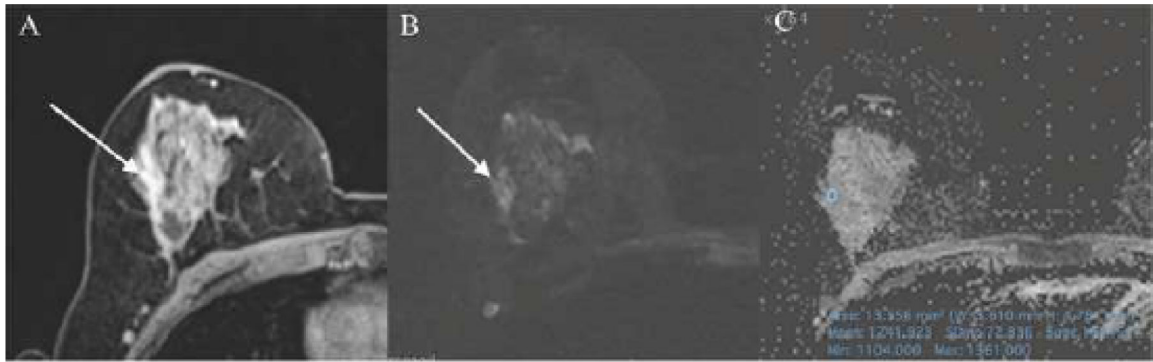d breast biopsy demonstrated columnar cell changes with atypia which remained benign on excisional breast biopsy. Except adapted mpMRI, which correctly classified this lesion as benign, all other approaches incorrectly classified the lesion as malignant.

Table 1.

Multiparametric MRI (mpMRI) protocol.

SEQUENCE	Plane	TR (ms)	TE (ms)	TI (ms)	FOV (mm)	SI	Slices	Matrix	Averages	b-value (s/mm^2)	TA
T2-weighted TSE imaging with fat suppression	axial	4800	61	230	340	4 mm	34	314 × 320	1		2:26 min
Three-acquisition trace DW, double-refocused single-shot EPI with inversion recovery fat suppression	axial	13700	83	220	340	3.5 mm	40	192 × 64 (50% oversampling)	2	50/850	3:19 min
DCE-MRI using a split-dynamics protocol [52] consisting of five alternating sections of high-spatial and high-temporal resolution T1-weighted sequences	High spatial resolution unenhanced coronal T1-weighted turbo FLASH-3D sequences without preparation pulse, with selective water-excitation	coronal	877	3.82		320	1 mm isotropic	96	320 × 134	1		2 min
	High temporal resolution coronal T1-weighted VIBE	coronal	3.61	1.4		320	1.7 mm isotropic	72	192 × 192	1		13.2 s per volume

Abbreviations: DCE-MRI, dynamic contrast-enhanced magnetic resonance imaging; DW, diffusion-weighted; EPI, echo-planar imaging; FLASH, fast-low-angle-shot; FOV, field of view; SI, signal intensity; TA, acquisition time; TE, echo time; TI, inversion time; TSE, turbo spin echo; TR, repetition time; VIBE, volume interpolated breath-hold examination

Table 2.

Histopathological characteristics of the non-mass enhancement lesions included in our investigation.

HISTOPATHOLOGY	n	%
Malignant	**39/66**	**59**
Ductal carcinoma in situ	4	10
Invasive Ductal Carcinoma	24	62
Invasive Lobular Carcinoma	9	23
IDC+DCIS	1	2.5
IDC+LCIS	1	2.5
Benign	**27/66**	**41**
FA/FAH	5	19
Adenosis, Sclerosing Adenosis, Focal Fibrosis, Apocrine metaplasia, Breast parenchyma, Fibrocystic changes	12	44
Papilloma	1	4
High-Risk (CCC with atypia, papilloma with atypia)	2	7
Other (chronic abscess, gynecomastia, fat necrosis, scar tissue)	7	26

[1]IDC = invasive ductal carcinoma; ILC = invasive lobular carcinoma; DCIS = ductal carcinoma in situ; FA = fibroadenoma; FAH = fibroadenomatoid hyperplasia; CCC = columnar cell changes.

Table 3.

Distribution and frequency of non-mass lesions according to the Breast Imaging Report and Data System (BI-RADS) descriptors.

		BENIGN n = 27 (41%)	MALIGNANT n = 39 (59%)
Distribution	Focal	13 (48%)	9 (23%)
	Linear	2 (7%)	4 (10%)
	Regional	9 (34%)	9 (23%)
	Segmental	2 (7%)	6 (15%)
	Multiple Regions	1 (4%)	8 (21%)
	Diffuse	-	3 (8%)
Pattern of Enhancement	Homogeneous	15 (56%)	17 (44%)
	Heterogenous	9 (33%)	14 (36%)
	Clumped	3 (11%)	6 (15%)
	Clustered Ring	-	2 (5%)
Kinetic Curve (Early Phase)	Slow	10 (37%)	6 (15%)
	Medium	10 (37%)	7 (18%)
	Fast	7 (26%)	26 (67%)
Kinetic Curve (Delayed Phase)	Persistent	15 (56%)	12 (31%)
	Plateau	11 (41%)	18 (46%)
	Wash-out	1 (3%)	9 (23%)

Table 4.

Mean ADC values for each reader and ADC values for the assigned BI-RADS category stratified by benign and malignant lesions

Characteristic	Benign, n = 27[a]	Malignant, n = 39[a]	p-value[b]
Reader1_ADC	1.40 (0.71, 2.46)	1.07 (0.59, 1.71)	< 0.001
Reader2_ADC	1.54 (1.13, 2.28)	1.06 (0.4, 1.65)	< 0.001
Reader1_ADC DCE BI-RADS 2	1.39 (0.72, 2.36)	n/a	
Reader1_ADC DCE BI-RADS 3	1.15	1.1 (0.66, 1.58)	
Reader1_ADC DCE BI-RADS 4	1.44 (1.06, 2.16)	1.18 (0.59, 1.71)	
Reader1_ADC DCE BI-RADS 5	n/a	1.03 (0.62, 1.69)	
Reader2_ADC DCE BI-RADS 2	1.77 (1.36, 2.28)	n/a	
Reader2_ADC DCE BI-RADS 3	1.43 (1.13, 1.94)	n/a	
Reader2_ADC DCE BI-RADS 4	1.25 (1.14, 1.43)	1.2 (0.55, 1.65)	
Reader2_ADC DCE BI-RADS 5	n/a	0.87 (0.4, 1.2)	

[a] Statistics presented: mean (minimum, maximum)

[b] Statistical tests performed: Wilcoxon rank-sum test

Table 5.

Sensitivity, specificity, PPV, NPV, diagnostic accuracy, and AUC for DCE, DWI using the determined best cut-off for each reader, and each mpMRI reading approach (EUSOBI mpMRI, 1.5 mpMRI, adapted mpMRI, and mpMRI individual threshold) for both readers. Significant differences before adjusting for multiple comparison are indicated.

READER	Modality	Sensitivity (95% CI)	Specificity (95% CI)	PPV (95% CI)	NPV (95% CI)	Accuracy (95% CI)
Reader 1	DCE	94.82 (82.72–99.44)	66.66 (45.98–83.38)	80.52 (66–90.64)	89.98 (68.2–98.78)	83.38 (72.16–91.3)
	DWI individual best threshold 1.215	74.36 (57.86–86.9)[†]	66.66 (45.98–83.38)	76.34 (59.84–88.66)	64.24 (44–81.4)	71.28 (58.74–81.62)
	EUSOBI mpMRI	84.7 (69.52–94.16)	55.66 (35.42–74.58)[‡]	73.26 (58.08–85.36)	71.5 (47.74–88.66)	72.82 (60.28–82.94)[‡]
	1.5 mpMRI	87.12 (72.6–95.7)	29.7 (13.86–50.16)[†‡*⊬◇]	64.24 (49.72–76.78)	61.6 (31.68–86.24)	63.58 (50.82–75.24)[†]
	adapted mpMRI	87.12 (72.6–95.7)	85.14 (66.22–95.92)[⊬]	89.54 (75.24–97.02)	82.06 (63.14–93.94)	86.46 (50.82–75.24)
	mpMRI individual best threshold 1.215	74.36 (57.86–86.9)[†]	66.66 (45.98–83.38)	76.34 (59.84–88.66)	64.24 (44–81.4)	71.28 (58.74–81.62)
Reader 2	DCE	100 (..–..)	77.88 (57.64–91.3)	86.68 (73.26–95.04)	100 (..–..)	90.86 (81.18–96.58)
	DWI individual best threshold 1.305	79.42 (63.58–90.64)	81.4 (61.82–93.72)	86.02 (70.4–95.26)	73.26 (54.12–87.78)	80.3 (68.64–89.1)
	EUSOBI mpMRI	77 (60.72–88.88)	81.4 (61.82–93.72)	85.8 (69.74–95.26)	71.06 (51.92–85.8)	78.76 (66.88–87.78)[†]
	1.5 MRI	94.82 (82.72–99.44)[‡*⊬◇]	40.7 (22.44–61.16)[†‡*⊬◇]	69.74 (55.66–81.62)	84.7 (54.56–98.12)	72.82 (60.28–82.94)[†]
	adapted mpMRI	71.72 (55.22–84.92)	85.14 (66.22–95.92)	87.56 (71.06–96.58)	67.54 (49.5–82.72)	77.22 (65.34–86.68)[†]
	mpMRI individual best threshold 1.305	79.42 (63.58–90.64)	81.4 (61.82–93.72)	86.02 (70.4–95.26)	73.26 (54.12–87.78)	80.3 (68.64–89.1)

[†]Significantly different from DCE-MRI (p < 0.05)

[‡]Significantly different from adapted mpMRI (p < 0.05)

[*]Significantly different from DWI individual best threshold (p < 0.05)

[⊬]Significantly different from EUSOBI mpMRI (p < 0.05)

[◇]Significantly different from mpMRI individual best threshold (p < 0.05)

Table 6.

False positive and false negative results for DCE, DWI using the determined best cut-off of each reader, EUSOBI mpMRI, 1.5 mpMRI, adapted mpMRI, and mpMRI individual threshold for each reader.

		DCE	DWI individual best threshold	EUSOBI mpMRI	1.5 mpMRI	Adapted mpMRI	mpMRI individual best threshold
Reader 1	False Negative	2	10	6	5	5	10
	False Positive	9	9	12	19	4	9
Reader 2	False Negative	0	8	9	2	11	8
	False Positive	6	5	5	16	4	5